AJNR

Quantitative Fiber Tracking Analysis of the Optic Radiation Correlated with Visual Performance in Premature Newborns

J.I. Berman, H.C. Glass, S.P. Miller, P. Mukherjee, D.M. Ferriero, A.J. Barkovich, D.B. Vigneron and R.G. Henry

ORIGINAL
RESEARCH

J.I. Berman
H.C. Glass
S.P. Miller
P. Mukherjee
D.M. Ferriero
A.J. Barkovich
D.B. Vigneron
R.G. Henry

Quantitative Fiber Tracking Analysis of the Optic Radiation Correlated with Visual Performance in Premature Newborns

BACKGROUND AND PURPOSE: Many prematurely born neonates have abnormalities of vision or visual processing. This study tests the hypothesis that a correlation exists between the microstructure of the optic radiation and visual performance in premature neonates.

MATERIALS AND METHODS: Diffusion tensor imaging (DTI) was performed on 36 premature neonates ranging in age from 29 to 41 weeks of gestational age (GA) at time of MR imaging. DTI fiber tracking methods were developed to delineate the optic radiations and segment the tract into anterior, middle, and posterior regions. Structural development and spatial heterogeneity in the delineated optic radiations were quantitatively assessed with diffusion tensor parameters including fractional anisotropy (FA), directionally averaged diffusivity (D_{av}), parallel diffusivity (λ_1), and transverse diffusivity ($\lambda_\perp$). Visual maturity of the preterm neonates at the time of MR imaging was assessed with a visual fixation task. Regression analysis was used to examine the relationship between neonatal visual performance and the microstructure of the optic radiation.

RESULTS: Fractional anisotropy within the optic radiation was observed to increase with GA ($P < .0001$). D_{av}, parallel diffusivity, and transverse diffusivity within the optic radiation each decreased with GA ($P < .0003$, $P < .02$, and $P < .0001$, respectively). The anterior segment of the optic radiation exhibited higher FA and lower D_{av}, parallel diffusivity, and transverse diffusivity ($P < .005$ each) than within the middle and posterior segments. Optic radiation fractional anisotropy correlated significantly with scores from the visual fixation tracking assessment, independent of GA ($P < .006$).

CONCLUSIONS: This study detected a significant link between the tissue architecture of the optic radiation and visual function in premature neonates.

Premature infants undergo a critical phase of rapid brain development in the weeks before term age. The white matter tracts are largely unmyelinated; however, the basic axonal connectivity of the major pathways is present in the premature brain.[1] The processes of axonal pathfinding, synaptogenesis, premyelination, and, finally, myelination begin during gestation and continue throughout infancy and adolescence.[2] However, brain maturation in the premature infant has been shown to be delayed as compared with term infants.[3,4] In addition, premature infants are susceptible to a variety of white matter injuries with little known effect on white matter development or long-term clinical outcome.[5-7] Many prematurely born neonates have abnormalities of vision or visual processing, which may be associated with these white matter injuries.[8]

This study used diffusion tensor MR imaging (DTI) to assess the microstructure of white matter within the optic radiations of premature neonates.[3,4,9-11] DTI fiber tracking has been used to study the development of white matter tracts in neonates with and without injury,[12-15] children with hemiparesis,[16] and infants with hypoxic ischemia.[17] This study seeks to link the microstructure of the developing optic radiation to premature neonatal visual performance and development. Understanding associations between noninvasive MR measurements and visual maturation in premature neonates will provide insight into developmental mechanisms and may be valuable for predicting abnormal development.

Materials and Methods

Imaging

Thirty-six premature infants were scanned with MR imaging. Our institution's review board approved this study, and we obtained parental consent for each neonate. Imaging was performed at 1.5T scanner (GE Medical Systems, Waukesha, Wis) with a custom-made high-sensitivity neonatal head coil integrated into an MR-compatible incubator.[18] The signal-to-noise ratio within the white matter on diffusion-weighted images was approximately 35, and the signal-to-noise ratio within white matter on the echo-planar images without diffusion weighting was approximately 65. At time of MR imaging, the infants ranged in age from 29 to 41 weeks of gestational age (GA) with a mean age of 34.5 weeks of GA. The infants were born at an average of 28.4 weeks of GA (range, 20.3–33.1 weeks' GA) and were scanned an average of 6.1 weeks after birth (range, 0.7–17 weeks). Neonates did not have severe periventricular white matter abnormalities on conventional T1- and T2-weighted images. With use of the grading system described previously,[6] 21 neonates had no periventricular white matter abnormalities, 9 neonates had minimal abnormalities, 4 had mild abnormalities, and 2 had moderate abnormalities. Three neonates had mild ventriculomegaly, and the remaining 33 neonates had no ventriculomegaly.
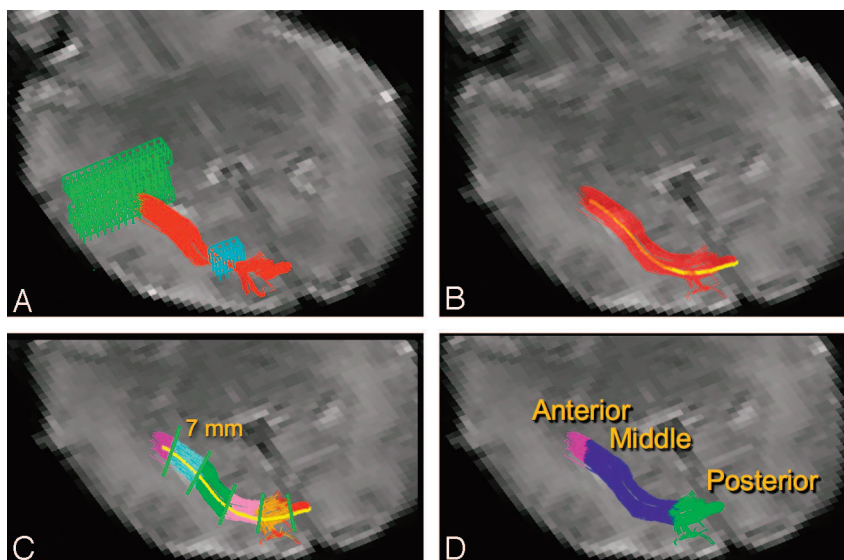
Fig 1. DTI fiber tracking and segmentation. *A*, DTI fiber tracks (*red*) were launched from a starting region of interest (*green mesh*) in a plane adjacent to the trigone of the lateral ventricle. Fiber tracks were filtered with a second region of interest (*blue mesh*) in a plane posterior to the lateral ventricle. *B*, The average fiber track (*yellow*) was constructed by averaging coordinates from each of the delineated optic radiation fiber tracks (*red*). *C*, The average fiber track was divided into 7-mm segments. Each voxel within the delineated optic radiation is assigned to the closest segment. Different segments are shown with various colors. *D*, Each discrete 7-mm segment is assigned to either the anterior, middle, or posterior anatomic segment of the optic radiation. The background image in each panel is an echo-planar image without diffusion weighting.

Diffusion tensor images were acquired with a 4.8-minute single-shot echo-planar sequence. Imaging parameters were TR, 7 s; TE, 100 ms; 256×128 matrix; 1.4×1.4 mm in-plane resolution; 3-mm-thick contiguous sections; 360- to 180-mm FOV; 167-kHz bandwidth; and 3 acquisition averages. Diffusion weighting gradients were applied in 6 noncolinear directions at $b = 600$ s/mm^2 in addition to a $b = 0$ s/mm^2 volume. A 2D 10th order nonlinear registration algorithm was used to correct for motion.[19,20] Diffusion-weighted volumes were adjusted to correct for motion with the $b = 0$ s/mm^2 volume used as a reference.

Before calculation of the diffusion tensor, a set of smoothed diffusion-weighted images was produced by averaging a 3×3 voxel in-plane neighborhood. The diffusion tensor and associated diffusion metrics were calculated for each voxel from the smoothed and unsmoothed diffusion-weighted images.[21] The smoothed diffusion metric maps were used for region-of-interest placement and DTI fiber tracking. To reduce partial volume averaging, we used the unsmoothed diffusion metric maps for tract-specific measurements.

Fiber Tracking and Quantification

We performed DTI fiber tracking and tract-specific quantification using software written with Interactive Data Language (ITT Visual Solutions, Boulder, Colo). The fiber tracking algorithm was based on the deterministic fiber tracking by the continuous assignment method.[22] The algorithm operates under the assumption that the primary eigenvector indicates the orientation of axonal bundles and follows the primary eigenvector from voxel to voxel in 3D. Fiber trajectories of the optic radiation are launched from a region of interest drawn on a plane anterior to the trigone of the lateral ventricle (Fig 1*A*). The starting region of interest spans multiple axial sections and was designed to include the entire white matter within and surrounding the optic radiation. DTI fiber tracks were initiated from 27 equally spaced starting points arranged in a $3 \times 3 \times 3$ grid within each voxel of the starting region. The fiber trajectories followed the primary eigenvector from voxel to voxel and were stopped when turning an unphysical angle of greater than 50° between 2 voxels or exiting the white matter

as indicated by fractional anisotropy (FA) less than 0.05. Fiber trajectories passing through a second region of interest drawn in a plane posterior to the lateral ventricle (Fig 1*A*) were retained as the delineated optic radiation. The second region of interest spans multiple axial sections containing the lateral ventricle and was designed to encompass the entire region of white matter that the optic radiation may pass through anterior to the visual cortex.

To examine the spatial heterogeneity of the optic radiation's microstructure, we segmented the delineated tracts into 3 anatomic regions. It is expected that diffusion metrics vary along the tract because of varying white matter geometry and architecture. The anterior region was defined as the portion of the optic radiation anterior to the lateral ventricle and closest to the thalamus. The middle region was adjacent to the lateral ventricle, and the posterior region was posterior to the ventricle and closest to the primary visual cortex. The steps in segmenting the delineated tract are shown in Fig 1. The first step (Fig 1*B*) in segmentation was to generate an average streamline or fiber track to characterize the position and curvature of the overall white matter tract. The average fiber track was calculated by averaging the coordinates of each step along each fiber trajectory. The second segmentation step (Fig 1*C*) was to divide the average fiber track into 7-mm-long segments starting with the lateral geniculate nucleus. Each fiber trajectory was then segmented such that each coordinate along the trajectory was assigned to the closest 7-mm segment. The final step (Fig 1*D*) involved a user manually assigning each of the 7-mm discrete segments to either the anterior, middle, or posterior anatomic segments.

Measurements of diffusion metrics including FA, eigenvalues (λ_1, λ_2, λ_3), and directionally averaged diffusivity (D_{av}) within the optic radiation were made on the basis of the voxels containing DTI fiber tracks. Transverse diffusivity, $\lambda_\perp$, is the mean of the second and third eigenvalues and indicates diffusivity perpendicular to axonal bundles. Tract-specific measurements were a weighted average with the number of fiber trajectories passing through a voxel comprising the weight for the voxel's DTI metric. Voxels with fewer fiber trajectories were assumed to include other unrelated white matter tracts and contrib-
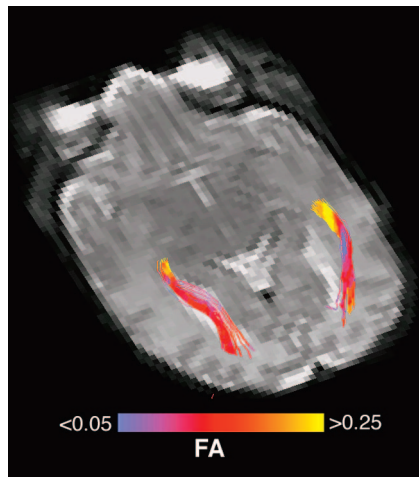
Fig 2. FA along optic radiation. Left and right optic radiations are shown in a 35-week GA premature infant. The fiber tracks originate in the thalamus and course posteriorly and adjacent to the ventricle toward the primary visual cortex. The fiber tracks are color coded by the underlying FA. The anterior portion of the tract is observed to have the highest FA.

ute less to the measurement. Voxels in the core of the white matter tract with many fiber trajectories contribute to most of the diffusion parameter measurements. Left- and right-sided optic radiation measurements within a patient were averaged. Measurements were taken from the entire optic radiation in addition to the anterior, middle, and posterior segments of the white matter tract.

Visual Function Examination

Each neonate was tested within 24 hours of MR imaging by the same child neurologist to assess visual function. The examiner was blinded to MR imaging results. The visual examination was performed when the neonate was in a maximally awake state with eyes open and limbs moving spontaneously. The neurologist's face was used as a target to test the infant's visual fixation and tracking ability once for a minimum of 2 consecutive minutes. Visual fixation tracking tests the integrity of the visual system, and test scores normally improve with increasing age.[23] The neonate's performance was scored from worst to best on a scale from 1 to 5. A score of 5 indicated stable fixation and complete following, a score of 4 indicated stable fixation and incomplete following, a score of 3 indicated stable fixation and rare following, a score of 2 indicated transient fixation and random eye movement, and a score of 1 indicated no fixation and random eye movements.

Results

DTI fiber tracks of the optic radiations were generated in each of the 36 premature infants included in this study. Figure 2 shows an example 3D view of the optic radiations in an infant scanned at 35 weeks of GA. The tract is observed to course adjacent to the ventricle to the visual cortex, corresponding to the known anatomy of the optic radiation. The spatial heterogeneity of the tract's FA is shown by color coding of the underlying FA values.

Tract-Specific Diffusion Metrics

Diffusion metrics were measured within the anterior, middle, and posterior segments of the optic radiation (Fig 3). FA within each anatomic segment significantly increased with age at an average rate of 6×10^{-3} ($\sim 3\%$) per week ($P < .0001$, Fig

3A). The rate of increase of FA with age was not significantly different among the 3 anatomic segments. FA within the 3 anatomic segments was significantly distinct ($P < .0001$, Wilcoxon signed-rank with Bonferroni correction), with the anterior segment exhibiting the highest FA and the posterior segment exhibiting the lowest FA.

The diffusivity metrics also exhibited correlations with age and anatomic segment. D_{av} decreased at an average rate of -17×10^{-6} mm^2/s per week ($P < .0003$). The primary eigenvalue, λ_1, decreased at an average rate of -10×10^{-6} mm^2/s per week ($P < .02$). Transverse diffusivity, $\lambda_\perp$, decreased with age at a rate of -21×10^{-6} mm^2/s per week ($P < .0001$). The rates of decrease between anatomic segments were not significantly different, and average rates for D_{av}, λ_1, and $\lambda_\perp$ are reported. The anterior segment of the optic radiation had significantly lower D_{av}, λ_1, and $\lambda_\perp$ compared with the middle and posterior segments ($P < .005$, Wicoxon signed rank with Bonferroni correction). The middle and posterior segments were not significantly differentiated by D_{av}, λ_1, or $\lambda_\perp$ measurements.

Diffusion Metrics and Functional Testing

The correlation between visual fixation performance and whole-tract diffusion metrics was analyzed while controlling for the effects of age with a multivariable regression. Optic radiation FA increased significantly with visual fixation score ($P < .006$) independent of GA (Fig 4). This relationship is most noticeable in the 2 infants older than 39 weeks of GA who exhibited poor visual fixation scores (3 and 4) and low FA for their age. Although D_{av}, λ_1, and $\lambda_\perp$ trended toward lower values with increased visual fixation score, the relationship did not reach significance.

Discussion

This study shows that quantitative DTI fiber tracking can link the microstructure of an unmyelinated white matter tract to function and behavior during a critical phase of brain development in preterm neonates. Visual function was assessed with a simple bedside ophthalmologic examination that did not require any specialized equipment. The quantitative fiber-tracking algorithm used a robust, multiple region-of-interest approach to delineate and segment the unmyelinated optic radiations of premature infants. This quantitative technique was capable of detecting spatial and temporal diffusion metric heterogeneities associated with the development and anatomy of the optic radiation.

In this study, DTI fiber tracking was used to delineate the preterm optic radiation in the same anatomic regions from previous histologic studies,[24] term equivalent aged infant fiber tracking studies,[14,25] and adult fiber tracking studies.[26,27] The 2-target region-of-interest method of fiber tracking used in this study is the same approach used in older populations. The axonal framework for the optic radiation's course from the lateral geniculate nucleus to the visual cortex is already present in premature infants. This axonal framework creates diffusion anisotropy but at a lower level than that observed in myelinated fibers. Therefore, the fractional anisotropy threshold is lowered for premature infant fiber tracking to enable delineation of unmyelinated white matter with low anisotropy.
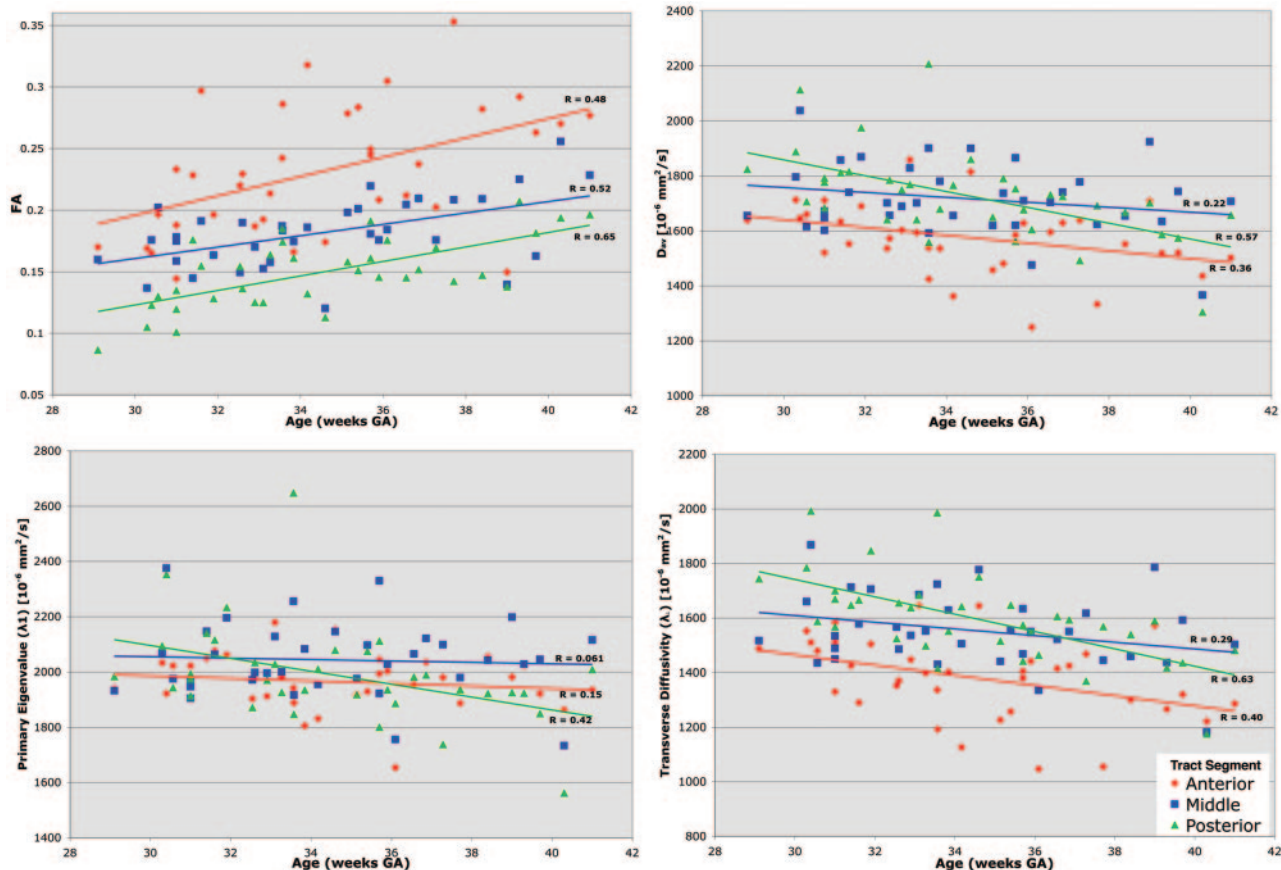
Fig 3. Tract-specific diffusion metrics. Plots show diffusion metrics (FA, D_{av}, λ_1, and $\lambda_\perp$) within the anterior (*red*), middle (*blue*), and posterior (*green*) segments of the optic radiation.
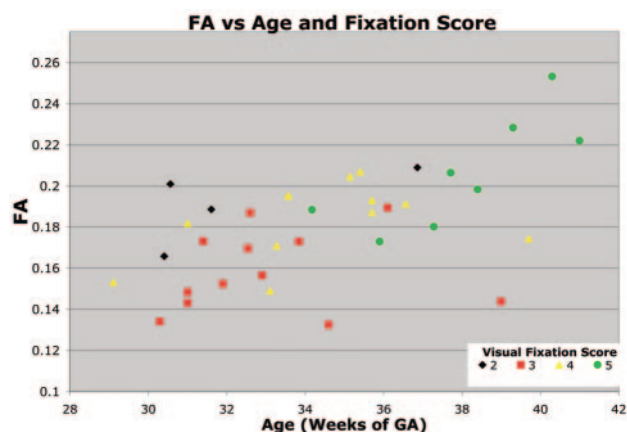

Fig 4. Relationship between visual fixation score, FA, and age. FA within the optic radiation increases with GA. The symbols are colored to indicate each neonate's visual fixation score on a scale from 1 to 5. Neonates with higher visual fixation scores demonstrated better visual fixation and tracking behavior. The visual fixation score correlated significantly with FA, independent of age. This relationship between visual fixation score and FA is evident within the set of neonates older than 39 weeks' GA. Two neonates older than 39 weeks' GA with abnormally poor visual examination performance also displayed abnormally low FA.

In the present study, the optic radiation was shown to have varying microstructural characteristics along its length. The anterior segment of the optic radiation closest to the thalamus exhibited highest FA and low diffusivity, indicating high axonal density within a compact fiber bundle. The middle segment was also a compact fiber bundle but exhibited lower FA and higher diffusivity than the anterior region. The difference in microstructure between the anterior and middle segments indicates possible early myelination within the anterior segment. The posterior segment of the optic radiation exhibited lowest FA because the optic radiation disperses near the visual cortex and intersects association and commissural tracts. Manually drawn regions of interest seek to sample a small homogeneous portion of a white matter tract and are not capable of quantitatively characterizing the structural heterogeneity along a 3D white matter tract.

This study detected age-related changes to the microstructure of the optic radiation associated with the structural maturation of the visual system. The diffusion metrics' means and rates of change observed in this fiber tracking study are in good agreement with those from previous premature infant studies which use manually drawn regions of interest.[11] This fiber tracking study focused on an early but limited age range between 29 and 41 weeks of GA. The trends in diffusion metrics observed in the unmyelinated preterm optic radiation represent an early stage of development that continues throughout infancy and childhood. The FA in the optic radiation is expected to continue to rise and diffusivity is expected to continue to decrease with functional and structural development, as shown in term infants[14] and throughout childhood.[28]

The results of this study demonstrate a correlation between visual performance and white matter microstructure during an early and critical phase of neurologic development. Previous studies showed that the visual fixation scores increase with

postmenstrual age and are lower in infants with focal white matter injury on T1-weighted imaging.[23] We now show that visual fixation scores are associated with FA such that premature neonates with lower scores have lower diffusion anisotropy. These results are independent of age, indicating that white matter microstructural integrity may mediate the effect of increasing age on the visual system. Low FA likely indicates low axonal fiber density, delayed premyelination, or increased water content. The correlation between preterm visual examination score and microstructure detected in our study is consistent with the results in the study by Bassi et al[25] of premature infants scanned at term equivalent age. The results from Bassi et al[25] and our study can be combined to gain an understanding of the relationship between white matter integrity and visual function during both gestation and infancy.

The visual fixation tracking scores assess the entire visual system, including structures and pathways that are not easily assessed with DTI and were not analyzed in this study. It is therefore possible that structural abnormalities outside of the optic radiation but within the visual system may also contribute to deficiencies in visual performance. Lower optic radiation FA values are associated with lower visual fixation scores; however, normal microstructure within the optic radiation as detected by DTI is not a guarantee of normal visual performance. Indeed, in this study, 2 preterm neonates older than 35 weeks of GA were observed to have normal optic radiation FA while performing poorly on the visual examination compared with other similarly aged neonates. Functional mapping techniques such as fMRI, EEG, and visual event-related potentials have been used to evaluate the visual function in adult and pediatric populations.[14,29-32] These techniques may provide additional visual system specificity but are still vulnerable to contributions or interference from unrelated adjacent brain structures. However, the combined results from the present premature infant study and previous adult and neonatal studies strongly support a connection between white matter microstructure and a wide range of visual system performance indicators.

Conclusions

This study shows the feasibility of use of DTI fiber tracking to delineate the optic radiation in premature neonates and measure changes to the tract's microstructure. This study suggests that infants with poor visual fixation scores for their age exhibit microstructural measures consistent with a delay in maturation of the optic radiation. These findings reinforce the close relationship between the structural integrity of a white matter tract and its function.

References

1. Kinney HC, Karthigasan J, Borenshteyn NI, et al. **Myelination in the developing human brain: biochemical correlates.** *Neurochem Res* 1994;19:983–96
2. Wimberger DM, Roberts TP, Barkovich AJ, et al. **Identification of "premyelination" by diffusion-weighted MRI.** *J Comput Assist Tomogr* 1995;19:28–33
3. Huppi PS, Maier SE, Peled S, et al. **Microstructural development of human newborn cerebral white matter assessed in vivo by diffusion tensor magnetic resonance imaging.** *Pediatr Res* 1998;44:584–90
4. Neil JJ, Shiran SI, McKinstry RC, et al. **Normal brain in human newborns: apparent diffusion coefficient and diffusion anisotropy measured by using diffusion tensor MR imaging.** *Radiology* 1998;209:57–66
5. Cioni G, Fazzi B, Coluccini M, et al. **Cerebral visual impairment in preterm infants with periventricular leukomalacia.** *Pediatr Neurol* 1997;17:331–38
6. Miller SP, Vigneron DB, Henry RG, et al. **Serial quantitative diffusion tensor MRI of the premature brain: development in newborns with and without injury.** *J Magn Reson Imaging* 2002;16:621–32
7. Woodward LJ, Anderson PJ, Austin NC, et al. **Neonatal MRI to predict neurodevelopmental outcomes in preterm infants.** *N Engl J Med* 2006;355:685–94
8. Pagliano E, Fedrizzi E, Erbetta A, et al. **Cognitive profiles and visuoperceptual abilities in preterm and term spastic diplegic children with periventricular leukomalacia.** *J Child Neurol* 2007;22:282–88
9. Basser PJ, Mattiello J, LeBihan, D. **Estimation of the effective self-diffusion tensor from the NMR spin echo.** *J Magn Reson B* 1994;103:247–54
10. Mukherjee P, Miller JH, Shimony JS, et al. **Normal brain maturation during childhood: developmental trends characterized with diffusion-tensor MR imaging.** *Radiology* 2001;221:349–58
11. Partridge SC, Mukherjee P, Henry RG, et al. **Diffusion tensor imaging: serial quantitation of white matter tract maturity in premature newborns.** *Neuroimage* 2004;22:1302–14
12. Berman, JI, Glass, HC, Miller SP, et al. **Quantitative fiber tracking analysis of the optic radiations in premature newborns.** Presented at the Joint Annual Meeting of the International Society for Magnetic Resonance in Medicine and the European Society for Magnetic Resonance in Medicine and Biology, Berlin, Germany, May 19–25, 2007.
13. Berman JI, Mukherjee P, Partridge SC, et al. **Quantitative diffusion tensor MRI fiber tractography of sensorimotor white matter development in premature infants.** *Neuroimage* 2005;27:862–71
14. Dubois J, Dehaene-Lambertz G, Soares C, et al. **Microstructural correlates of infant functional development: example of the visual pathways.** *J Neurosci* 2008;28:1943–48
15. Partridge SC, Vigneron DB, Charlton NN, et al. **Pyramidal tract maturation after brain injury in newborns with heart disease.** *Ann Neurol* 2006;59:640–51
16. Glenn OA, Henry RG, Berman JI, et al. **DTI-based three-dimensional tractography detects differences in the pyramidal tracts of infants and children with congenital hemiparesis.** *J Magn Reson Imaging* 2003;18:641–48
17. van Pul C, Buijs J, Vilanova A, et al. **Infants with perinatal hypoxic ischemia: feasibility of fiber tracking at birth and 3 months.** *Radiology* 2006;240:203–14
18. Dumoulin CL, Rohling KW, Piel JE, et al. **Magnetic resonance imaging compatible neonate incubator.** *Magn Reson Engineering* 2002;15:117–28
19. Woods RP, Grafton ST, Holmes CJ, et al. **Automated image registration: I. General methods and intrasubject, intramodality validation.** *J Comput Assist Tomogr* 1998;22:139–52
20. Woods RP, Grafton ST, Watson JD, et al. **Automated image registration: II. Intersubject validation of linear and nonlinear models.** *J Comput Assist Tomogr* 1998;22:153–65
21. Basser PJ, Pierpaoli, C. **Microstructural and physiological features of tissues elucidated by quantitative-diffusion-tensor MRI.** *J Magn Reson Series B* 1996;111:209–19
22. Mori S, Crain BJ, Chacko VP, et al. **Three-dimensional tracking of axonal projections in the brain by magnetic resonance imaging.** *Ann Neurol* 1999;45:265–69
23. Glass HC, Fujimoto S, Ceppi-Cozzio C, et al. **White-matter injury is associated with impaired gaze in premature infants.** *Pediatr Neurol* 2008;38:10–15
24. Burgel U, Amunts K, Hoemke L, et al. **White matter fiber tracts of the human brain: three-dimensional mapping at microscopic resolution, topography and intersubject variability.** *Neuroimage* 2006;29:1092–1105
25. Bassi L, Ricci D, Volzone A, et al. **Probabilistic diffusion tractography of the optic radiations and visual function in preterm infants at term equivalent age.** *Brain* 2008;131:573–82
26. Toosy AT, Ciccarelli O, Parker GJ, et al. **Characterizing function-structure relationships in the human visual system with functional MRI and diffusion tensor imaging.** *Neuroimage* 2004;21:1452–63
27. Yamamoto A, Miki Y, Urayama S, et al. **Diffusion tensor fiber tractography of the optic radiation: analysis with 6-, 12-, 40-, and 81-directional motion-probing gradients, a preliminary study.** *AJNR Am J Neuroradiol* 2007;28:92–96
28. Mukherjee P, Miller JH, Shimony JS, et al. **Diffusion-tensor MR imaging of gray and white matter development during normal human brain maturation.** *AJNR Am J Neuroradiol* 2002;23:1445–56
29. Biagioni E, Frisone MF, Laroche S, et al. **Maturation of cerebral electrical activity and development of cortical folding in young very preterm infants.** *Clin Neurophysiol* 2007;118:53–59
30. Seghier ML, Lazeyras F, Zimine S, et al. **Visual recovery after perinatal stroke evidenced by functional and diffusion MRI: case report.** *BMC Neurol* 2005;5:17
31. Shimony JS, Burton H, Epstein AA, et al. **Diffusion tensor imaging reveals white matter reorganization in early blind humans.** *Cereb Cortex* 2006;16:1653–61
32. Taoka T, Sakamoto M, Iwasaki S, et al. **Diffusion tensor imaging in cases with visual field defect after anterior temporal lobectomy.** *AJNR Am J Neuroradiol* 2005;26:797–803